I&EC research
Industrial & Engineering Chemistry Research

ACS Editors' Choice

Article

pubs.acs.org/IECR

Terms of Use

Solubility of CO_2 and CH_4 in Ionic Liquids: Ideal CO_2/CH_4 Selectivity

Mahinder Ramdin,[†] Aris Amplianitis,[†] Stepan Bazhenov,[‡] Alexey Volkov,[‡] Vladimir Volkov,[‡,¶] Thijs J.H. Vlugt,*[,†] and Theo W. de Loos[†]

[†]Engineering Thermodynamics, Process & Energy Department, Faculty of Mechanical, Maritime and Materials Engineering, Delft University of Technology, Leeghwaterstraat 39, 2628 CB Delft, The Netherlands

[‡]A.V. Topchiev Institute of Petrochemical Synthesis, Russian Academy of Sciences, Leninsky prospect 29, Moscow 119991, Russian Federation

[¶]National Research Nuclear University MEPhI, Kashirskoye shosse 31, Moscow 115409, Russian Federation

Supporting Information

ABSTRACT: A synthetic method has been used to measure the bubble-point pressures of carbon dioxide (CO_2) and methane (CH_4), for a temperature range of 303.15−363.15 K and for pressures up to 14 MPa, in the following ionic liquids: 1-ethyl-3-methylimidazolium diethylphosphate [emim][dep], trihexyltetradecylphosphonium bis(2,4,4-trimethylpentyl)phosphinate [thtdp][phos], trihexyltetradecylphosphonium dicyanamide [thtdp][dca], 1-allyl-3-methylimidazolium dicyanamide [amim][dca], 1-butyl-1-methylpyrrolidinium dicyanamide [bmpyrr][dca], 1,2,3-tris(diethylamino)cyclopropenylium dicyanamide [cprop][dca], 1,2,3-tris(diethylamino)cyclopropenylium bis(trifluoromethylsulfonyl)imide [cprop][Tf_2N], 1-butyl-1-methylpiperidinium bis(trifluoromethylsulfonyl)imide [bmpip][Tf_2N], triethylsulfonium bis(trifluoromethylsulfonyl)imide [tes][Tf_2N], and methyltrioctylammonium bis(trifluoromethylsulfonyl)imide [toa][Tf_2N]. The solubility of CH_4 on mole fraction basis is a factor of 10 lower than that of CO_2 at similar conditions. Henry constants of CO_2 and CH_4 in all the ionic liquid (IL) systems are presented, from which the ideal CO_2/CH_4 selectivities are obtained. The ideal CO_2/CH_4 selectivities of the investigated ILs are in the range of the conventional solvents like Selexol, Purisol, Rectisol, Fluor Solvent, and sulfolane. The ideal CO_2/CH_4 selectivity decreases dramatically with increasing temperature and increasing IL molecular weight. Furthermore, the experimental data has been modeled accurately with the Peng−Robinson equation of state in combination with van der Waals mixing rules.

1. INTRODUCTION

Natural gas contains a variety of impurities including the sour gases carbon dioxide (CO_2) and hydrogen sulfide (H_2S).[1,2] These sour gases have to be removed in order to meet customer specifications and to avoid technical problems during gas transportation. CO_2 should be eliminated because of its low caloric value and because of the risk of dry ice formation during the liquefaction of natural gas. H_2S concentrations should be reduced drastically to avoid pipeline corrosion.[3] The sweetening of the natural gas is typically performed in an absorber−stripper configuration using either a physical solvent, a chemical solvent, or a mixture of both depending on the type and concentration of the impurities.[1] Despite the inherent high pressure of the sweetening process, which is favorable for physical absorption purposes, the majority of the units in the field utilize chemical solvents (e.g., monoethanolamine (MEA)).[4] The use of physical solvents (e.g., Purisol, Rectisol, Selexol, etc.) is not uncommon in the natural gas industry and is in fact preferred over chemical solvents at high acid gas partial pressures.[1] The selection of the proper solvent for natural gas sweetening is not trivial because it depends on many factors (e.g., composition, temperature and partial pressures of the acid gases, and product specifications). For guidelines, the reader is referred to the work of Tennyson and Schaaf[1] and Kohl and Nielsen.[2] Although the aqueous amine process is effective at removing acid gas components from natural gas for a wide range of conditions, it suffers a number of serious drawbacks. These include the high energy requirement for solvent regeneration, the low CO_2/H_2S selectivity, the corrosivity, and the volatility of the used amines.[5] Therefore, many researchers have posed alternatives to overcome some of the problems associated with the amine process. In the past few years, ionic liquids (ILs), which are salts with melting points lower than 100 °C and characterized by very low vapor pressures, have emerged as a promising solvent for acid gas removal.[3,6] In the past decade, a large number of studies reported the solubility of CO_2 and, to a lesser extent, of other acid gas components in many different kinds of ionic liquids.[4,7] In practice, however, not the solubility but the selectivity of one component toward the another is more important for judging the separation performance of an absorption process.[4] This implies that a potential IL for natural gas sweetening should not only have a high individual CO_2 and H_2S solubility but at the same time also a low CH_4 solubility. In other words, the IL should have a high CO_2/CH_4 and CO_2/H_2S selectivity. Lei et al.[7] provide an excellent review of the solubility of different gases in ILs, whereas Karadas et al.,[3] Ramdin et al.[4] and Kumar et al.[6] review the application potential of ILs for natural gas sweetening. Recently, Mortazavi-Manesh et al.[8] used the

Special Issue: Alírio Rodrigues Festschrift

Received: December 11, 2013
Revised: February 12, 2014
Accepted: February 12, 2014
Published: February 12, 2014

COSMO-RS model to screen more than 400 ILs for the separation of acid gases. Unfortunately, the amount of experimental data on CO_2/CH_4 and CO_2/H_2S selectivities in ILs are extremely scarce, which is mainly due to the high toxicity of H_2S for the latter system, but this reason is less obvious for the CO_2/CH_4 system.

This motivated us to study CO_2 and CH_4 solubilities and CO_2/CH_4 (ideal) selectivities in a total of 10 ILs composed of 8 different classes of cations and 4 different types of anions. A synthetic method has been used to measure the bubble-point pressures of CO_2 and CH_4, for a temperature range of 303.15−363.15 K and for pressures up to 14 MPa, in the following ionic liquids: 1-ethyl-3-methylimidazolium diethylphosphate [emim][dep], trihexyltetradecylphosphonium bis(2,4,4-trimethylpentyl)phosphinate [thtdp][phos], trihexyltetradecylphosphonium dicyanamide [thtdp][dca], 1-allyl-3-methylimidazolium dicyanamide [amim][dca], 1-butyl-1-methylpyrrolidinium dicyanamide [bmpyrr][dca], 1,2,3-tris(diethylamino)cyclopropenylium dicyanamide [cprop][dca], 1,2,3-tris(diethylamino)cyclopropenylium bis(trifluoromethylsulfonyl)imide [cprop][Tf_2N], 1-butyl-1-methylpiperidinium bis(trifluoromethylsulfonyl)imide [bmpip][Tf_2N], triethylsulfonium bis(trifluoromethylsulfonyl)imide [tes][Tf_2N], and methyltrioctylammonium bis(trifluoromethylsulfonyl)imide [toa][Tf_2N]. The experimental data has been reduced by calculating the Henry constants from which the ideal CO_2/CH_4 selectivities are obtained. The ideal CO_2/CH_4 selectivities of the investigated ILs are compared with those of conventional solvents used in the natural gas industry. Furthermore, the experimental data has been modeled with the Peng−Robinson equation of state in combination with van der Waals mixing rules.

2. EXPERIMENTAL SECTION

The gases CO_2 and CH_4 used in the experiments had a purity of 99.995 mol % and were purchased from the Linde Group. The ILs, purchased from Sigma-Aldrich, were always dried in vacuo at a temperature of 80 °C for several days before usage. The molecular structures of the investigated ILs are shown in Figure 1. The water content of the ILs after drying was determined by Karl Fischer titration, and the results together with other properties are shown in Table 1. Note that the purity of the ILs reported in Table 1 is prior to drying, whereas the water content is only measured and reported after the drying step. The ILs contained typically 1−2% water; therefore, the actual purity of the ILs will always be higher than the reported values. The VLE experiments start with filling a Pyrex glass tube with a known amount of IL. This tube is then connected to a gas-dosing system, which is used to degas the IL and to dose a known amount of gas into the tube using mercury as a displacement fluid. The exact amount of gas is calculated through the virial equation of state truncated after the second term.[9] Subsequently, the tube with a known composition is disconnected from the gas-dosing system and placed in the Cailletet apparatus. Here, only a brief description of the Cailletet apparatus will be presented because a detailed explanation of the experimental procedure can be found elsewhere.[10] The Cailletet apparatus allows phase equilibria measurements in a temperature and pressure range of 255−470 K and 0.1−15 MPa, respectively. For a binary system at bubble point conditions, the Gibbs phase rule unequivocally requires two independent variables to be fixed. Therefore, the composition and the temperature were fixed in the experiments, and the pressure was gradually increased until the disappearance of the last bubble in the liquid (i.e., the bubble-point pressure). The VLE measurements then involve the determination of bubble-point pressures at different, but fixed, compositions and temperatures. The pressure is obtained by a dead weight gauge, and the temperature is controlled by a thermostatic bath equipped with a Pt-100 (ASL F250) thermometer. The standard uncertainty in the experimental pressure, temperature, and composition is ±0.005 MPa, ± 0.01 K (i.e., the fluctuations in temperature were within the accuracy

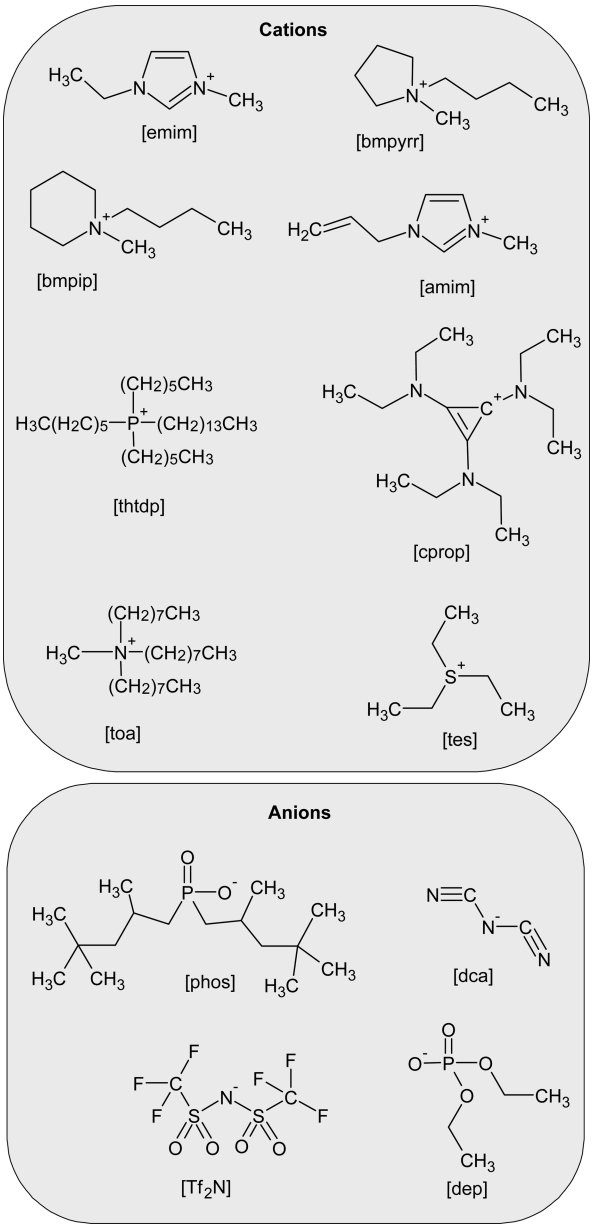

Figure 1. Cations and anions of the investigated ILs. Abbreviation cations: 1-allyl-3-methylimidazolium [amim], 1-ethyl-3-methylimidazolium [emim], 1,2,3-tris(diethylamino)cyclopropenylium [cprop], 1-butyl-1-methylpiperidinium [bmpip], 1-butyl-1-methylpyrrolidinium [bmpyrr], methyltrioctylammonium [toa], trihexyltetradecylphosphonium [thtdp], and triethylsulfonium [tes]. Abbreviation anions: bis(trifluoromethylsulfonyl)imide [Tf_2N], dicyanamide [dca], bis(2,4,4-trimethylpentyl)phosphinate [phos], and diethylphosphate [dep].

dx.doi.org/10.1021/ie4042017 | Ind. Eng. Chem. Res. 2014, 53, 15427−15435

Table 1. Properties of the Used ILs[a]

name of the IL (abbreviation)	molecular weight (g/mol)	purity[b] (mole %)	water content[c] (ppm)
[emim][dep]	264.26	≥98.0	<250
[thtdp][phos]	773.27	≥95.0	<350
[thtdp][dca]	549.90	≥95.0	<350
[amim][dca]	189.22	≥98.5	<200
[bmpyrr][dca]	208.30	≥97.0	<200
[cprop][dca]	318.46	≥96.5	<200
[cprop][Tf_2N]	532.56	≥96.5	<150
[bmpip][Tf_2N]	436.43	≥96.5	<150
[tes][Tf_2N]	399.39	≥99.0	<150
[toa][Tf_2N]	648.85	≥99.0	<150

[a]The water content was measured with Karl Fischer titration, whereas the purities were reported by the supplier (Sigma-Aldrich).[27] [b]Purity of ILs before drying. [c]Water content of ILs after drying.

of the thermometer), and ±0.003 in the mole fraction, respectively.

3. THERMODYNAMIC MODELING

The Peng–Robinson (PR) equation of state[11] (EoS) has been applied to model the experimental data

$$P = \frac{RT}{v - b_m} - \frac{a_m}{v(v + b_m) + b_m(v - b_m)} \quad (1)$$

where v is the molar volume and a_m and b_m are constants for the mixture accounting for the molecular interaction and covolume, respectively. The PR EoS is used in combination with the quadratic van der Waals (vdW) mixing rules[9]

$$a_m = \sum_i \sum_j x_i x_j a_{ij} \quad a_{ij} = \sqrt{a_i a_j}(1 - k_{ij}) \quad k_{ii} = k_{jj} = 0 \quad (2)$$

$$b_m = \sum_i \sum_j x_i x_j b_{ij} \quad b_{ij} = \frac{1}{2}(b_i + b_j)(1 - l_{ij}) \quad l_{ii} = l_{jj} = 0 \quad (3)$$

where k_{ij} and l_{ij} represent the binary interaction parameters and a_i and b_i the pure component parameters accounting for molecular interaction and covolume, respectively. Calculation of the pure component parameters requires the critical properties and acentric factors of all the components participating in the mixture. These properties are not known (i.e., not experimentally available) for ILs because many ILs start to decompose before reaching the critical point. Therefore, one has to rely on group-contribution methods,[12] molecular simulations,[13,14] or suitable correlations.[15] Here, the modified Lydersen–Joback–Reid group-contribution method proposed by Valderrama et al.[12] is used to obtain the critical properties of all the investigated ILs. The critical parameters and acentric factors of all the ILs are listed in Table 2. Once these properties have been obtained, the PR EoS can readily be applied to calculate the bubble point of the gas–IL systems. The binary interaction parameters k_{ij} and l_{ij} are simultaneously optimized using a simplex algorithm in MATLAB[16] minimizing the objective function

$$\mathrm{OF} = \frac{1}{N}\sum_{i=1}^{N}\left|\frac{P_i^{\mathrm{exp}} - P_i^{\mathrm{pred}}}{P_i^{\mathrm{exp}}}\right| \quad (4)$$

Table 2. Critical Temperature (T_c), Pressure (P_c), and Acentric Factor (ω) of the Components Used in the Modeling

component	T_c (K)	P_c (MPa)	ω
[emim][dep][a]	877.2	2.147	0.722
[thtdp][phos][a]	1878.8	0.551	−0.139
[thtdp][dca][a]	1525.5	0.765	0.582
[amim][dca][a]	1019.2	2.799	0.788
[bmpyrr][dca][a]	887.2	2.061	0.855
[cprop][dca][a]	1073.7	1.615	1.073
[cprop][Tf_2N][a]	1255.7	1.803	0.588
[bmpip][Tf_2N][a]	1108.0	2.264	0.392
[tes][Tf_2N][a]	1189.9	2.190	0.160
[toa][Tf_2N][a]	1376.1	1.064	0.996
CH_4[b]	190.6	4.599	0.012
CO_2[b]	304.12	7.374	0.225

[a]Calculated using the method of Valderrama et al.[12] [b]Taken from Poling et al.[28]

where N is the number of experimental points, P_i^{exp} and P_i^{pred} the experimental and predicted bubble-point pressure, respectively.

4. RESULTS AND DISCUSSION

Due to space constraints, only a selection of the data will be presented here. The raw experimental data and extensive P vs T and P vs x diagrams of all the systems can be found in the Supporting Information. A comparison of the CO_2 solubility in the investigated ILs is shown in Figure 2. The CO_2 + IL systems show a typical behavior: the solubility increases with increasing pressure and decreases with increasing temperature. The solubility trend, on a mole fraction basis, observed for CO_2 obeys the following order: [thtdp][phos] > [toa][Tf2N] > [thtdp][dca] > [cprop][Tf2N] > [bmpip][Tf2N] > [tes]-[Tf2N] > [cprop][dca] > [emim][dep] > [bmpyrr][dca] > [amim][dca]. However, this trend completely vanishes if the solubility is compared on a molality basis, indicating a strong molecular weight effect. The data more or less collapse on the

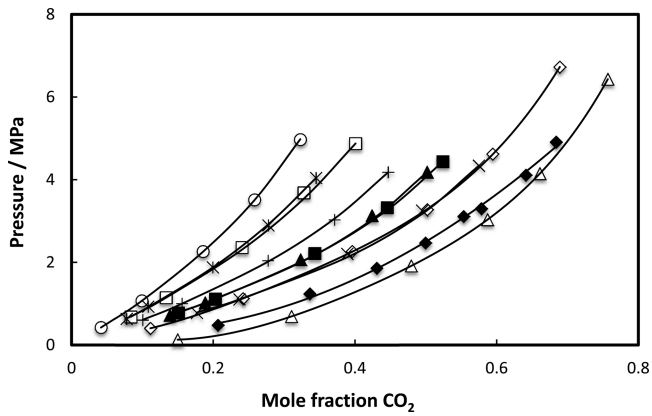

Figure 2. Comparison of CO_2 solubility at 313.15 K in the investigated ILs: [emim][dep] (open squares), [thtdp][phos] (open triangles),[29] [thtdp][dca] (open diamonds),[29] [amim][dca] (open circles), [bmpyrr][dca] (stars), [cprop][dca] (plusses), [cprop][Tf_2N] (crosses), [bmpip][Tf_2N] (closed squares), [tes][Tf_2N] (closed triangles), and [toa][Tf_2N] (closed diamonds).[30] The lines are the PR EoS modeling results using the parameters of the critical properties in Table 2.

dx.doi.org/10.1021/ie4042017 | Ind. Eng. Chem. Res. 2014, 53, 15427−15435

universal solubility curve proposed by Carvalho and Coutinho[17] as can be seen in Figure 3. The behavior of CH_4 is similar to

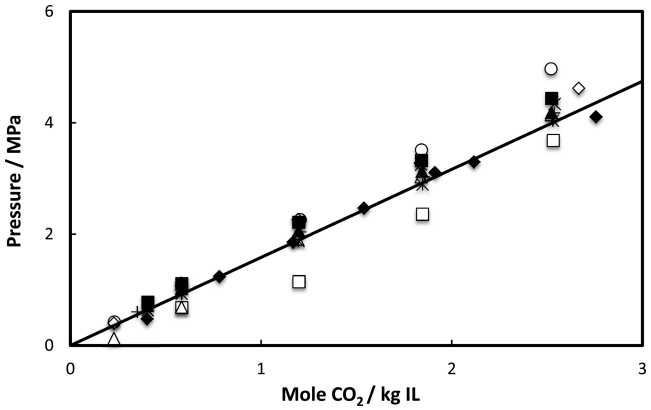

Figure 3. Comparison of CO_2 solubility on molality scale at 313.15 K in the investigated ILs: [emim][dep] (open squares), [thtdp][phos] (open triangles),[29] [thtdp][dca] (open diamonds),[29] [amim][dca] (open circles), [bmpyrr][dca] (stars), [cprop][dca] (plusses), [cprop][Tf_2N] (crosses), [bmpip][Tf_2N] (closed squares), [tes]-[Tf_2N] (closed triangles), and [toa][Tf_2N] (closed diamonds).[30] The line is the correlation by Carvalho and Coutinho.[17]

that of CO_2, but the solubility of CH_4 is an order of magnitude lower compared to CO_2 at similar conditions (see Figure 4). It

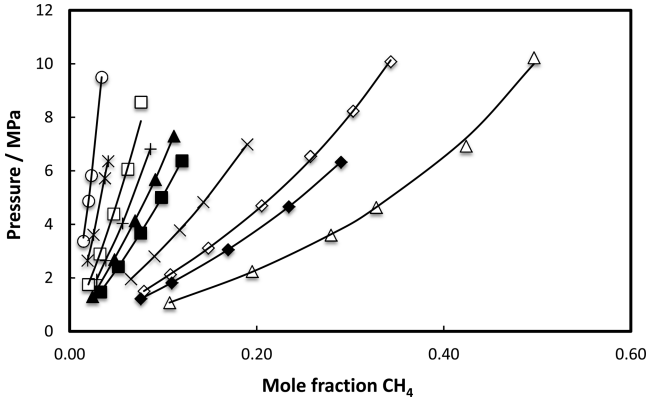

Figure 4. Comparison of CH_4 solubility at 313.15 K in the investigated ILs: [emim][dep] (open squares), [thtdp][phos] (open triangles),[29] [thtdp][dca] (open diamonds),[29] [amim][dca] (open circles), [bmpyrr][dca] (stars), [cprop][dca] (plusses), [cprop][Tf_2N] (crosses), [bmpip][Tf_2N] (closed squares), [tes][Tf_2N] (closed triangles), and [toa][Tf_2N] (closed diamonds).[30] The lines are PR EoS modeling results using the parameters in Table 2

is surprising to see that the data for CH_4 do not collapse on an universal absorption curve as in the case of CO_2 (see Figure 5). The CH_4 solubility is higher in ILs containing large nonpolar alkyl-chains, which obviously interacts with the nonpolar CH_4 molecule (i.e., the "like dissolve like" principle). As explained earlier, in practice, not the solubility but the selectivity is the key parameter for judging the separation performance. There are several ways to obtain the ideal selectivity, ($S^{I}_{i/j}$), from VLE data. The first approach to calculate the selectivity is to use the liquid-phase mole fractions of the individual gases at a constant temperature and pressure (see eq 5)

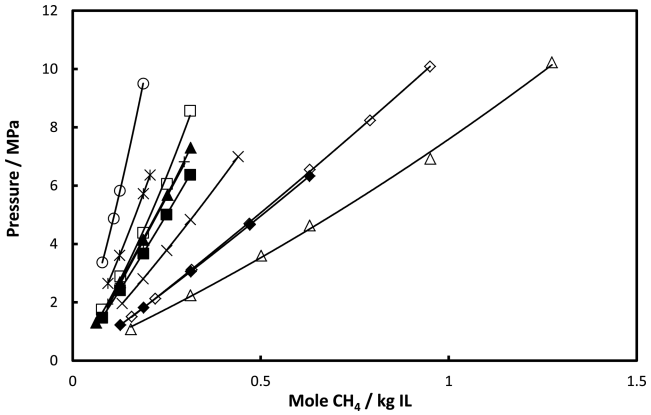

Figure 5. Comparison of CH_4 solubility on molality scale at 313.15 K in the investigated ILs: [emim][dep] (open squares), [thtdp][phos] (open triangles),[29] [thtdp][dca] (open diamonds),[29] [amim][dca] (open circles), [bmpyrr][dca] (stars), [cprop][dca] (plusses), [cprop][Tf_2N] (crosses), [bmpip][Tf_2N] (closed squares), [tes]-[Tf_2N] (closed triangles), and [toa][Tf_2N] (closed diamonds).[30] The lines are polynomial fits to guide the eye.

$$S^{I}_{CO_2/CH_4} = \left(\frac{x_{CO_2}}{x_{CH_4}}\right)_{P,T} \tag{5}$$

The second approach is to use the ratio of the bubble-point pressures at a constant temperature and composition as given in eq 6

$$S^{I}_{CO_2/CH_4} = \left(\frac{P_{CH_4}}{P_{CO_2}}\right)_{T,x} \tag{6}$$

The third approach is to use the ratio of the Henry constants of CH_4 over that of CO_2

$$S^{I}_{CO_2/CH_4} = \left(\frac{H_{CH_4}}{H_{CO_2}}\right) \tag{7}$$

In principle, the ideal selectivity will be different depending on which of the above equations are used for the calculations. For convenience, we will use eq 7 for all the ideal selectivity calculations because eqs 5 and 6 will require interpolations or extrapolations and because the data of CO_2 and CH_4 are generally not measured at the same mole fraction or pressure. The Henry constants, H_{12}, are calculated as

$$H_{12} = \lim_{x_1 \to 0} \frac{f_1^L}{x_1} \tag{8}$$

The fugacity, f_1^L, of the solute "1" (either CO_2 or CH_4) in the solvent "2" is calculated using a suitable equation of state for CO_2[18] and CH_4[19] assuming pure CO_2 or CH_4 in the gas phase and applying the equilibrium condition $f_1^L = f_1^V$. The calculated Henry constants for CO_2 and CH_4 in all the ILs are listed in Tables 3 and 4, respectively. The Henry constants (solubility) increase (decreases) with increasing temperature for both CO_2 and CH_4 systems. Henry constants for the systems CO_2–[emim][dep] and CO_2–[tes][Tf_2N] have been reported by Palgunadi et al.[20] and Nonthanasin et al.,[21] respectively. The values for Henry constants reported in Table 3 agree within 10% of the literature data (e.g., the Henry constant of CO_2 in [tes][Tf_2N] reported by Nonthanasin et al. is 4.5 MPa at 313

dx.doi.org/10.1021/ie4042017 | Ind. Eng. Chem. Res. 2014, 53, 15427−15435

Table 3. Henry Constants (H_{12}/MPa) of CO_2 (1) in the Investigated ILs (2) Obtained by Plotting the Fugacity versus the Mole Fraction and Taking the Limit of $x_1 \rightarrow 0$

	temperature (K)						
name of the IL (abbreviation)	303.15	313.15	323.15	333.15	343.15	353.15	363.15
[emim][dep]	6.53	7.91	9.38	10.95	12.60	14.35	16.19
[thtdp][phos][a]		0.71	0.86	1.08	1.37	1.73	2.16
[thtdp][dca][a]	3.00	3.58	4.14	4.67	5.18	5.68	6.15
[amim][dca]	8.19	10.04	11.99	14.02	16.16	18.386	20.707
[bmpyrr][dca]	6.62	7.96	9.44	11.07	12.84	14.77	16.85
[cprop][dca]	4.98	5.88	6.82	7.82	8.88	9.99	11.15
[cprop][Tf2N]	3.61	4.26	4.94	5.65	6.40	7.19	8.01
[bmpip][Tf2N]	4.19	5.01	5.88	6.81	7.79	8.83	9.92
[tes][Tf2N]	4.20	5.03	5.93	6.89	7.93	9.02	10.19
[toa][Tf2N][b]	1.67	2.28	2.89	3.49	4.05		

[a]Data taken from Ramdin et al.[29] [b]Calculated from Nam and Lee.[30]

Table 4. Henry Constants (H_{12}/MPa) of CH_4 (1) in the Investigated ILs (2) Obtained by Plotting the Fugacity versus the Mole Fraction and Taking the Limit of $x_1 \rightarrow 0$

	temperature (K)						
name of the IL (abbreviation)	303.15	313.15	323.15	333.15	343.15	353.15	363.15
[emim][dep]	82.02	85.79	89.26	92.42	95.26	97.77	99.96
[thtdp][phos]	9.38	9.92	10.42	10.89	11.32	11.72	12.09
[thtdp][dca]	18.02	18.95	19.83	20.66	21.42	22.12	22.76
[amim][dca]	216.3	218.94	220.97	222.4	223.23	223.46	223.1
[bmpyrr][dca]	128.36	133.25	137.65	141.55	144.95	147.82	150.18
[cprop][dca]	63.56	65.35	66.92	68.27	69.40	70.30	70.97
[cprop][Tf_2N]	27.87	29.03	30.12	31.13	32.07	32.94	33.73
[bmpip][Tf_2N]	41.77	43.93	45.94	47.80	49.50	51.04	52.42
[tes][Tf_2N]	50.22	52.34	54.33	56.20	57.94	59.55	61.03
[toa][Tf_2N]	15.06	15.84	16.60	17.32	18.01	18.66	19.28

Table 5. Gibbs Energy ($\Delta_{abs}G$), Enthalpy ($\Delta_{abs}H$), and Entropy of Absorption ($\Delta_{abs}S$) of CO_2 in the ILs[a]

CO_2 + IL	$\Delta_{abs}G$ (kJ mol^{-1})	$\Delta_{abs}H$ (kJ mol^{-1})	$\Delta_{abs}S$ (J mol^{-1} K^{-1})
[emim][dep]	11.4	−14.7	−83.2
[thtdp][phos][b]	5.1	−12.5	−56.1
[thtdp][dca][b]	9.3	−13.1	−71.5
[amim][dca]	12.0	−15.4	−87.4
[bmpyrr][dca]	11.4	−14.4	−82.4
[cprop][dca]	10.6	−12.7	−74.5
[cpop][Tf_2N]	9.8	−12.7	−71.7
[bmpip][Tf_2N]	10.2	−13.7	−76.3
[tes][Tf_2N]	10.2	−14.0	−77.2
[toa][Tf_2N][c]	8.1	−22.3	−97.1

[a]The values of $\Delta_{abs}G$, $\Delta_{abs}H$, and $\Delta_{abs}S$ are consistent with a reference state of 0.1 MPa and 313.15 K. [b]Calculated from Ramdin et al.[29] [c]Calculated from Nam and Lee.[30]

K, which is slightly lower than the 5.0 MPa reported here). The deviation in the Henry constants is likely due to errors using eq 8 as the extrapolation $x_1 \rightarrow 0$ is performed. Information on the dissolution behavior at the molecular level can be obtained by calculating the enthalpy and entropy of absorption of the solute in the solvent. These properties are closely related to the strength of the interaction between the solute and the solvent and the degree of ordering of the solvent molecules around a solute molecule, respectively. The calculation of the Gibbs energy, the enthalpy, and entropy of absorption requires an appropriate correlation of the Henry constants as a function of temperature. Therefore, the temperature dependency of the Henry constant was fitted to the Benson−Krause (BK) equation[22]

$$\ln[H_{12}/\mathrm{MPa}] = \sum_{i=0}^{m} a_i (T/\mathrm{K})^{-i} \tag{9}$$

Using the BK equation, the Gibbs energy, the enthalpy, and the entropy of absorption of the solute in the IL can be calculated using the thermodynamic relations[23]

$$\Delta_{abs}G^{\infty} = RT[\ln(H_{12})] \tag{10}$$

$$\Delta_{abs}H^{\infty} = -T^2\left[\frac{\partial}{\partial T}\left(\frac{\Delta_{abs}G^{\infty}}{T}\right)\right] = -RT^2\left[\frac{\partial \ln(H_{12})}{\partial T}\right] \tag{11}$$

dx.doi.org/10.1021/ie4042017 | Ind. Eng. Chem. Res. 2014, 53, 15427−15435

Table 6. Gibbs Energy ($\Delta_{abs}G$), Enthalpy ($\Delta_{abs}H$), and Entropy of Absorption ($\Delta_{abs}S$) of CH_4 in the ILs[a]

CH_4 + IL	$\Delta_{abs}G$ (kJ mol^{-1})	$\Delta_{abs}H$ (kJ mol^{-1})	$\Delta_{abs}S$ (J mol^{-1} K^{-1})
[emim][dep]	17.6	−3.5	−67.2
[thtdp][phos]	12.0	−4.3	−51.9
[thtdp][dca]	13.7	−3.9	−56.1
[amim][dca]	20.0	−0.9	−66.8
[bmpyrr][dca]	18.7	−2.9	−69.0
[cprop][dca]	16.9	−2.1	−60.7
[cpop][Tf_2N]	14.8	−3.2	−57.3
[bmpip][Tf_2N]	15.8	−3.9	−63.0
[tes][Tf_2N]	16.3	−3.2	−62.3
[toa][Tf_2N]	13.2	−4.0	−54.8

[a]The values of $\Delta_{abs}G$, $\Delta_{abs}H$, and $\Delta_{abs}S$ are consistent with a reference state of 0.1 MPa and 313.15 K.

Table 7. Ideal CO_2/CH_4 Selectivity Obtained by Calculating the Ratio of the Henry Constants of CH_4 over CO_2

	temperature (K)						
name of the IL (abbreviation)	303.15	313.15	323.15	333.15	343.15	353.15	363.15
[emim][dep]	12.6	10.8	9.5	8.4	7.6	6.8	6.2
[thtdp][phos]		14.0	12.1	10.1	8.3	6.8	5.6
[thtdp][dca]	6.0	5.3	4.8	4.4	4.1	3.9	3.7
[amim][dca]	26.4	21.8	18.4	15.9	13.8	12.2	10.8
[bmpyrr][dca]	19.4	16.7	14.6	12.8	11.3	10.0	8.9
[cprop][dca]	12.8	11.1	9.8	8.7	7.8	7.0	6.4
[cprop][Tf_2N]	7.7	6.8	6.1	5.5	5.0	4.6	4.2
[bmpip][Tf_2N]	10.0	8.8	7.8	7.0	6.4	5.8	5.3
[tes][Tf_2N]	12.0	10.4	9.2	8.2	7.3	6.6	6.0
[toa][Tf_2N]	9.0	7.0	5.8	5.0	4.4		

$$\Delta_{abs}S^{\infty} = \frac{(\Delta_{abs}H^{\infty} - \Delta_{abs}G^{\infty})}{T} = -RT\left[\frac{\partial \ln(H_{12})}{\partial T}\right] - R\ln(H_{12}) \quad (12)$$

The calculated properties of CO_2 and CH_4 are listed in Tables 5 and 6, respectively. The negative value of the enthalpy of absorption of CO_2 and CH_4 indicates that the dissolution process is exothermic, and the higher values of CO_2 compared to those of CH_4 are consistent with the higher solubilities of CO_2. However, the solubility trend of CO_2 observed in the ILs cannot solely be explained by solute−solvent interactions. For example, the enthalpy of absorption of CO_2 in [amim][dca] is higher (i.e., stronger interaction) than that in [thtdp][phos], whereas the solubility of CO_2 is much lower in the former IL. The solubility trend can be explained by the entropic effects, which dominate the dissolution behavior of CO_2 in the ILs. This is completely opposite for CH_4, as can be seen in Table 6. The CH_4 solubility trend observed in the ILs is consistent with the enthalpy of absorption values reported in Table 6. The enthalpy of absorption of CH_4 is higher for ILs containing long nonpolar alkyl chains, which is due to nonpolar−nonpolar interactions. This suggests that the solute−solvent interactions dominate the dissolution of CH_4, but entropic effects are much more important for CO_2.

Subsequently, the ideal CO_2/CH_4 selectivities are calculated using eq 7, and the results are presented in Table 7. Interestingly, the ideal selectivity decreases rapidly with increasing temperature for all the investigated systems. However, Figure 6 shows that this trend is not unique for IL systems; it also holds for conventional solvents like Selexol, Purisol, Rectisol, Fluor Solvent, and sulfolane. The reason for this dramatic reduction of selectivity at higher temperatures is that the methane solubility is only slightly influenced by the temperature, whereas the effect for CO_2 is much larger. The consequence of this is that the Henry constant of CH_4 is nearly independent of temperature, whereas the Henry constant of CO_2 increases rapidly with temperature. Nevertheless, some of the ILs (e.g., [amim][dca] and [bmpyrr][dca]) perform better in terms of ideal selectivities than most of the conventional solvents. Moreover, the ideal selectivity decreases, with some exceptions, with increasing IL molecular weight (see Table 8

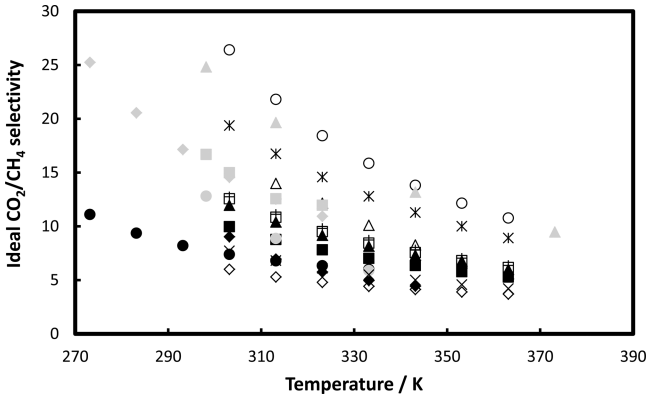

Figure 6. Comparison of the ideal CO_2/CH_4 selectivity in the investigated ILs and in conventional solvents at 313.15 K: [emim]-[dep] (open squares), [thtdp][phos] (open triangles), [thtdp][dca] (open diamonds), [amim][dca] (open circles), [bmpyrr][dca] (stars), [cprop][dca] (plusses), [cprop][Tf_2N] (crosses), [bmpip][Tf_2N] (black squares), [tes][Tf_2N] (black triangles), [toa][Tf_2N] (black diamonds), Rectisol (black circles), Fluor Solvent (gray squares), Sulfolane (gray triangles), Purisol (gray diamonds), and Selexol (gray circles). Data of conventional solvents taken from refs 37−48

dx.doi.org/10.1021/ie4042017 | Ind. Eng. Chem. Res. 2014, 53, 15427−15435

Table 8. Effect of IL Molecular Weight on the Ideal CO_2/CH_4 Selectivity at 313.15 K

name of the IL (abbreviation)	molecular weight (g/mol)	selectivity (CO_2/CH_4)	reference
[emim][dep]	264.26	10.8	this work
[thtdp][phos]	773.27	14.0	this work
[thtdp][dca]	549.90	5.3	this work
[amim][dca]	189.22	21.8	this work
[bmpyrr][dca]	208.30	16.7	this work
[cprop][dca]	318.46	11.1	this work
[cprop][Tf_2N]	532.56	6.8	this work
[bmpip][Tf_2N]	436.43	8.8	this work
[tes][Tf_2N]	399.39	10.4	this work
[toa][Tf_2N]	648.85	7.0	this work
[hmpy][Tf_2N]	458.43	10.8	31
[thtdp][Tf_2N]	764.00	6.2	32
[bmim][Tf_2N]	419.36	18.5	32
[hmim][Tf_2N]	447.42	8.1	32−34
[emim][dca]	177.21	21.0	33,34
[emim][CF_3SO_3]	260.23	17.3	33,34
[emim][Tf_2N]	391.31	11.2	33,34
[mmim][$MeSO_4$]	208.24	17.6	33,34
[emim][BF_4]	197.97	20.0	33,34
[bmim][BF_4]	226.02	14.9	23
[bmim][PF_6]	284.18	12.2	23
[bmim][$MeSO_4$]	250.32	14.1	35
[emim][FAP]	556.17	9.7	36

and Figure 7). This suggests that a low molecular weight IL should be used if a high selectivity is desired, which is consistent with the findings of Camper et al.[24] and Scovazzo,[25] because molar volumes of ILs generally increases with increasing IL molecular weight.[4] Unfortunately, the CO_2 solubility on mole fraction basis is not very high for low molecular weight ILs. In conclusion, there is a trade off between solubility, which increases with IL molecular weight, and selectivity, which decreases with increasing IL molecular weight.

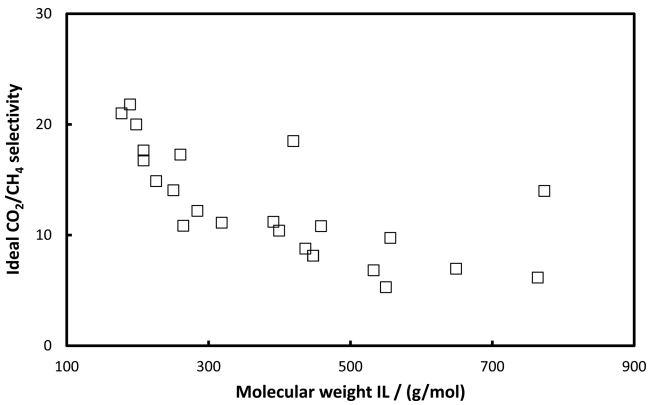

Figure 7. Effect of IL molecular weight on the ideal CO_2/CH_4 selectivity at 313.15 K.

However, the poor CO_2/CH_4 selectivity for higher molecular weight ILs is not a surprise because the molecular weight of the ILs is mainly increased by adding alkyl groups. The obvious consequence of this is that the CH_4 solubility increases as the number or length of the nonpolar alkyl chains increases.

So far, we have considered the ideal CO_2/CH_4 selectivities, but in the real natural gas sweetening process, which operates at high pressures, nonidealities are likely to occur. Consequently, the real selectivities will probably differ from the ideal selectivities. Because measurements of mixed-gas solubilities are more difficult, almost no CO_2−CH_4−IL mixture data can be found in the literature. Hert et al.[26] reported the solubility of the binary gas mixture CO_2−CH_4 in the IL [hmim][Tf_2N] and concluded that the solubility of the sparingly soluble CH_4 is enhanced in the presence of CO_2. This indicates that in a real process, which typically contains many gaseous components in the feed, interaction and competition between different solutes may influence the dissolution process. In a subsequent study, we will provide solubility data and a thorough discussion of CO_2−CH_4 mixtures in several ILs.

5. CONCLUSIONS

The solubility of CO_2 and CH_4 has been measured in the following ionic liquids: 1-ethyl-3-methylimidazolium diethylphosphate [emim][dep], trihexyltetradecylphosphonium bis(2,4,4-trimethylpentyl)phosphinate [thtdp][phos], trihexyltetradecylphosphonium dicyanamide [thtdp][dca], 1-allyl-3-methylimidazolium dicyanamide [amim][dca], 1-butyl-1-methylpyrrolidinium dicyanamide [bmpyrr][dca], 1,2,3-tris(diethylamino)cyclopropenylium dicyanamide [cprop][dca], 1,2,3-tris(diethylamino)cyclopropenylium bis(trifluoromethylsulfonyl)imide [cprop][Tf_2N], 1-butyl-1-methylpiperidinium bis(trifluoromethylsulfonyl)imide [bmpip][Tf_2N], triethylsulfonium bis(trifluoromethylsulfonyl)imide [tes][Tf_2N], and methyltrioctylammonium bis(trifluoromethylsulfonyl)imide [toa][Tf_2N]. The solubility data has been reduced by calculating the Henry constants of CO_2 and CH_4 in all the ILs, from which the ideal CO_2/CH_4 selectivities are obtained. The ideal CO_2/CH_4 selectivities of the investigated ILs are in the range of the conventional solvents like Selexol, Purisol, Rectisol, Fluor Solvent, and sulfolane. The ideal CO_2/CH_4 selectivity decreases with increasing temperature and increasing IL molecular weight. Therefore, a low molecular weight IL should be used if a high selectivity is desired. Furthermore, the experimental data has been modeled accurately with the Peng−Robinson equation of state in combination with van der Waals mixing rules.

■ ASSOCIATED CONTENT

Supporting Information

Extensive tables containing raw experimental data, P vs T and P vs x diagrams including PR EoS modeling results of all the investigated systems. This material is available free of charge via the Internet at http://pubs.acs.org/.

■ AUTHOR INFORMATION

Corresponding Author

*T. J. H. Vlugt. E-mail: t.j.h.vlugt@tudelft.nl.

Notes

The authors declare no competing financial interest.

■ ACKNOWLEDGMENTS

Financial support by the ADEM, A green Deal in Energy Materials, program of the Dutch Ministry of Economic Affairs, Agriculture and Innovation. The authors thank Ir. E. J. M. Straver for his assistance with the experimental work. This research cooperation is also a part of Dutch−Russian Centre of Excellence "Gas4S" (NWO-RFBR No. 047.018.2006.014/08-08-92890-CE).

■ REFERENCES

(1) Tennyson, R. N.; Schaaf, R. P. Guidelines can help choose proper process for gas-treating plants. *Oil Gas J.* **1977**, *75*, 78−86.
(2) Kohl, A. L.; Nielsen, R. B. *Gas Purification*; Gulf Publishing Company: Houston, TX, 1997.
(3) Karadas, F.; Atilhan, M.; Aparicio, S. Review on the Use of Ionic Liquids (ILs) as Alternative Fluids for CO_2 Capture and Natural Gas Sweetening. *Energy Fuels* **2010**, *24*, 5817−5828.
(4) Ramdin, M.; de Loos, T. W.; Vlugt, T. J. H. State-of-the-Art of CO_2 Capture with Ionic Liquids. *Ind. Eng. Chem. Res.* **2012**, *51*, 8149−8177.
(5) D'Alessandro, D. M.; Smit, B.; Long, J. R. Carbon Dioxide Capture: Prospects for New Materials. *Angew. Chem., Int. Ed.* **2010**, *49*, 6058−6082.
(6) Kumar, S.; Cho, J. H.; Moon, I. Ionic liquid-amine blends and CO2BOLs: Prospective solvents for natural gas sweetening and CO_2 capture technology-A review. *Int. J. Greenhouse Gas Control* **2014**, *20*, 87−116.
(7) Lei, Z.; Dai, C.; Chen, B. Gas Solubility in Ionic Liquids. *Chem. Rev.* **2014**, *114*, 1289−1326.
(8) Mortazavi-Manesh, S.; Satyro, M. A.; Marriott, R. A. Screening Ionic Liquids as Candidates for Separation of Acid Gases: Solubility of Hydrogen Sulfide, Methane, and Ethane. *AIChE J.* **2013**, *59*, 2993−3005.
(9) Prausnitz, J. M.; Lichtenthaler, R. N.; Gomes de Azevedo, E. *Molecular Thermodynamics of Fluid-Phase Equilibria*, 3rd ed.; Prentice Hall PTR: Upper Saddle River, NJ, 1999.
(10) de Loos, T. W.; van der Kooi, H. J.; Ott, P. L. Vapor-Liquid Critical Curve of the System Ethane + 2-Methylpropane. *J. Chem. Eng. Data* **1986**, *31*, 166−168.
(11) Peng, D.; Robinson, D. B. A New Two-Constant Equation of State. *Ind. Eng. Chem. Fundam.* **1976**, *15*, 59−64.
(12) Valderamma, J. O.; Rojas, R. E. Critical Properties of Ionic Liquids. Revisited. *Ind. Eng. Chem. Res.* **2009**, *48*, 6890−6900.
(13) Rai, N.; Maginn, E. J. Vapor-Liquid Coexistence and Critical Behavior of Ionic Liquids via Molecular Simulations. *J. Phys. Chem. Lett.* **2011**, *2*, 1439−1443.
(14) Rai, N.; Maginn, E. J. Critical behaviour and vapour-liquid coexistence of 1-alkyl-3-methylimidazolium bis-(trifluoromethylsulfonyl)amide ionic liquids via Monte Carlo simulations. *Faraday Discuss.* **2012**, *154*, 53−69.
(15) Rebelo, L. O. N.; Canongia Lopes, J. N.; Esperanca, J. M. S. S.; Filipe, E. On the Critical Temperature, Normal Boiling Point, and Vapor Pressure of Ionic Liquids. *J. Phys. Chem. B* **2005**, *109*, 6040−6043.
(16) Martin, A.; Bermejo, M. D.; Mato, F. A.; Cocero, M. J. Teaching advanced equations of state in applied thermodynamics courses using open source programs. *Educ. Chem. Eng.* **2011**, *6*, e114−e121.
(17) Carvalho, P. J.; Coutinho, J. A. P. On the Nonideality of CO_2 Solutions in Ionic Liquids and Other Low Volatile Solvents. *J. Phys. Chem. Lett.* **2010**, *1*, 774−780.
(18) Span, R.; Wagner, W. A New Equation of State for Carbon Dioxide Covering the Fluid Region from the Triple-Point Temperature to 1100 K at Pressures up to 800 MPa. *J. Phys. Chem. Ref. Data* **1996**, *25*, 1509−1596.
(19) Setzmann, U.; Wagner, W. A New Equation of State and Tables of Thermodynamic Properties for Methane Covering the Range from the Melting Line to 625 K at Pressures up to 1000 MPa. *J. Phys. Chem. Ref. Data* **1991**, *20*, 1061−1155.
(20) Palgunadi, J.; Kang, J. E.; Nguyen, D. Q.; Kim, J. H.; Min, B. K.; Lee, S. D.; Kim, H. S. Solubility of CO_2 in dialkylimidazolium dialkylphosphate ionic liquids. *Thermochim. Acta* **2009**, *494*, 94−98.
(21) Nonthanasin, T.; Henni, A.; Saiwan, C. Densities and low pressure solubilities of carbon dioxide in five promising ionic liquids. *RSC Adv.* **2014**, *4*, 7566−7578.
(22) Benson, B. B.; Krause, D. Empirical laws for dilute aqueous solutions of nonpolar gases. *J. Chem. Phys.* **1976**, *64*, 689−709.
(23) Jacquemin, J.; Costa Gomes, M. F.; Husson, P.; Majer, V. Solubility of carbon dioxide, ethane, methane, oxygen, nitrogen, hydrogen, argon, and carbon monoxide in 1-butyl-3-methylimidazolium tetrafluoroborate between temperatures 283 and 343 K and at pressures close to atmospheric. *J. Chem. Thermodyn.* **2006**, *38*, 490−502.
(24) Camper, D.; Bara, J.; Koval, C.; Noble, R. Bulk-Fluid Solubility and Membrane Feasibility of Rmim-Based Room-Temperature Ionic Liquids. *Ind. Eng. Chem. Res.* **2006**, *45*, 6279−6283.
(25) Scovazzo, P. Determination of the upper limits, benchmarks, and critical properties for gas separations using stabilized room temperature ionic liquid membranes (SILMs) for the purpose of guiding future research. *J. Membr. Sci.* **2009**, *343*, 199−211.
(26) Hert, D. G.; Anderson, J. L.; Aki, S. N. V. K.; Brennecke, J. F. Enhancement of oxygen and methane solubility in 1-hexyl-3-methylimidazolium bis(trifluoromethylsulfonyl) imide using carbon dioxide. *Chem. Commun.* **2005**, 2603−2605.
(27) Sigma-Aldrich. http://www.sigmaaldrich.com/chemistry/chemistry-products.html?TablePage=16255866 (accessed Nov 27, 2013).
(28) Poling, B. E.; Prausnitz, J. M.; O'Connell, J. P. *The Properties of Gases and Liquids*, 5th ed.; Mc Graw Hill: Singapore, 2007.
(29) Ramdin, M.; Zuzuarregui Olasagasti, T.; Vlugt, T. J. H.; de Loos, T. High pressure solubility of CO_2 in non-fluorinated phosphonium-based ionic liquids. *J. Supercrit. Fluids* **2013**, *82*, 41−49.
(30) Nam, S. G.; Lee, B. Solubility of carbon dioxide in ammonium-based ionic liquids: Butyltrimethylammonium bis-(trifluoromethylsulfonyl)imide and methyltrioctylammonium bis-(trifluoromethylsulfonyl)imide. *Korean J. Chem. Eng.* **2013**, *30*, 474−481.
(31) Anderson, J. L.; Dixon, J. K.; Brennecke, J. F. Solubility of CO_2, CH_2, C_2H_6, C_2H_4, O_2 and N_2 in 1-Hexyl-3-methylpyridinium Bis(trifluoromethylsulfonyl)imide: Comparison to Other Ionic Liquids. *Acc. Chem. Res.* **2007**, *40*, 1208−1216.
(32) Carvalho, P. J.; Coutinho, J. A. P. The polarity effect upon the methane solubility in ionic liquids: a contribution for the design of ionic liquids for enhanced CO_2/CH_4 and H_2S/CH_4 selectivities. *Energy Environ. Sci.* **2011**, *4*, 4614−4619.
(33) Finotello, A.; Bara, J. E.; Narayan, S.; Camper, D.; Noble, R. D. Ideal Gas Solubilities and Solubility Selectivities in a Binary Mixture of Room-Temperature Ionic Liquids. *J. Phys. Chem. B* **2008**, *112*, 2335−2339.
(34) Finotello, A.; Bara, J. E.; Camper, D.; Noble, R. D. Room-Temperature Ionic Liquids: Temperature Dependence of Gas Solubility Selectivity. *Ind. Eng. Chem. Res.* **2008**, *47*, 3453−3459.
(35) Kumelan, J.; Perez-Salado Kamps, A.; Tuma, D.; Maurer, G. Solubility of the Single Gases Methane and Xenon in the Ionic Liquid [bmim][CH_3SO_4]. *J. Chem. Eng. Data* **2007**, *52*, 2319−2324.
(36) Althuluth, M.; Kroon, M. C.; Peters, C. J. Solubility of Methane in the Ionic Liquid 1-Ethyl-3-methylimidazolium Tris-(pentafluoroethyl)trifluorophosphate. *Ind. Eng. Chem. Res.* **2012**, *51*, 16709−16712.
(37) Henni, A.; Tontiwachwuthikul, P.; Chakma, A. Solubility Study of Methane and Ethane in Promising Physical Solvents for Natural Gas Sweetening Operations. *J. Chem. Eng. Data* **2006**, *51*, 64−67.
(38) Rayer, A. V.; Henni, A.; Tontiwachwuthikul, P. High Pressure Physical Solubility of Carbon Dioxide (CO_2) in Mixed Polyethylene Glycol Dimethyl Ethers (Genosorb 1753). *Can. J. Chem. Eng.* **2012**, *90*, 576−583.
(39) Rayer, A. V.; Henni, A.; Tontiwachwuthikul, P. High-Pressure Solubility of Methane (CH_4) and Ethane (C_2H_6) in Mixed

Polyethylene Glycol Dimethyl Ethers (Genosorb 1753) and Its Selectivity in Natural Gas Sweetening Operations. *J. Chem. Eng. Data* **2012**, *57*, 764−775.
(40) Henni, A.; Tontiwachwuthikul, P.; Chakma, A. Solubilities of Carbon Dioxide in Polyethylene Glycol Ethers. *Can. J. Chem. Eng.* **2005**, *83*, 358−361.
(41) Miyano, Y.; Fujihara, I. Henry's constants of carbon dioxide in methanol at 250−500 K. *Fluid Phase Equilib.* **2004**, *221*, 57−62.
(42) Jou, F. Y.; Deshmukh, R. D.; Otto, F. D.; Mather, A. E. Solubility of H_2S, CO_2, CH_4 and C_2H_6 in Sulfolane at elevated pressures. *Fluid Phase Equilib.* **1990**, *56*, 313−324.
(43) Melzer, W. M.; Schrodter, F.; Knapp, H. Solubilities of Methane, Propane and Carbon Dioxide in solvent mixtures consisting of water, N,N-Dimethylformamide, and N-methyl-2-pyrrolidone. *Fluid Phase Equilib.* **1989**, *49*, 167−186.
(44) Rivas, O. R.; Prausnitz, J. M. Sweetening of Sour Natural Gases by Mixed-Solvent Absorption: Solubilities of Ethane, Carbon Dioxide, and Hydrogen Sulfide in Mixtures of Physical and Chemical Solvents. *AIChE J.* **1979**, *25*, 975−984.
(45) Murrieta-Guevara, F.; Romero-Martinez, A.; Trejo, A. Solubilities of Carbon Dioxide and Hydrogen Sulfide in Propylene Carbonate, N-methylpyrrolidone and Sulfolane. *Fluid Phase Equilib.* **1998**, *44*, 105−115.
(46) Xu, Y.; Schutte, R. P.; Hepler, L. G. Solubilities of Carbon Dioxide, Hydrogen Sulfide and Sulfur Dioxide in Physical Solvents. *Can. J. Chem. Eng.* **1992**, *70*, 569−573.
(47) Schnabel, T.; Vrabec, J.; Hasse, H. Molecular simulation study of hydrogen bonding mixtures and new molecular models for mono- and dimethylamine. *Fluid Phase Equilib.* **2008**, *63*, 144−159.
(48) Wu, Y.; Carroll, J. J.; Zhu, W. *Sour Gas and Related Technologies*; Wiley: Toronto, Canada, 2012.